Nonpolar *a*-plane light-emitting diode with an *in-situ* SiN_x interlayer on *r*-plane sapphire grown by metal-organic chemical vapour deposition*

Fang Hao(方 浩), Long Hao(龙 浩), Sang Li-Wen(桑立雯), Qi Sheng-Li(齐胜利), Xiong Chang(熊 畅), Yu Tong-Jun(于彤军)†, Yang Zhi-Jian(杨志坚), and Zhang Guo-Yi(张国义)

State Key Laboratory of Artificial Microstructure and Mesoscopic Physics, School of Physics, Peking University, Beijing 100871, *China*

(Received 3 January 2010; revised manuscript received 3 February 2010)

We report on the growth and fabrication of nonpolar *a*-plane light emitting diodes with an *in-situ* SiN_x interlayer grown between the undoped *a*-plane GaN buffer and Si-doped GaN layer. X-ray diffraction shows that the crystalline quality of the GaN buffer layer is greatly improved with the introduction of the SiN_x interlayer. The electrical properties are also improved. For example, electron mobility and sheet resistance are reduced from high resistance to 31.6 $cm^2/(V \cdot s)$ and 460 $\Omega/\square$ respectively. Owing to the significant effect of the SiN_x interlayer, *a*-plane LEDs are realized. Electroluminescence of a nonpolar *a*-plane light-emitting diode with a wavelength of 488nm is demonstrated. The emission peak remains constant when the injection current increases to over 20 mA.

Keywords: metal-organic chemical deposition, III-nitrides, nonpolar, light emitting diodes

PACS: 78.70.Ch, 78.55.Cr, 78.60.Fi, 78.67.De **DOI:** 10.1088/1674-1056/20/1/017804

1. Introduction

The current commercial technology for blue–green light emitting diodes (LEDs) employs GaN films grown in the polar *c*-direction. It is well known that *c*-plane LEDs undergo the quantum-confined Stark effect,[1,2] which is induced by a strong spontaneous and piezoelectric polarization electric field.[3] The efficiency and luminescent output power of the device are both decreased due to the smaller overlap of electron and hole wavefuctions caused by the built-in electric fields along the *c*-direction. A large electric field also results in a red-shift of LED emission.[4] As a potential means of eliminating the effects of polarization fields in devices of III-nitrides, *a*-plane GaN material[5−8] and multiple quantum wells (MQWs)[9,10] have become more and more attractive in recent years. However, as the crystalline quality of *a*-plane GaN grown on *r*-plane sapphire substrates is lower than that of their counterparts on *c*-plane sapphire, *a*-plane LEDs on *r*-plane sapphire are hard to fabricate and relevant studies are seldom reported.[11,12] High-density defects in the GaN films limit the performance of LEDs because threading dislocations act as nonradiative recombination centres and reduce the radiative recombination efficiency. Lateral epitaxial overgrowth and the SiN_x interlayer have been employed for achieving defect reduction in *a*-GaN. As an *in-situ* growth technique, the SiN_x interlayer has proven to be an effective and convenient method.[13−15] A SiN_x nanomask, which is grown between the undoped *a*-plane GaN buffer and Si-doped GaN layer, can switch the growth mode from two-dimensional (2D) to three-dimensionnal (3D) temporarily. By controlling the growth conditions, epitaxial layer overgrowth takes place on the random SiN_x nanomask pattern. This 2D–3D–2D process could significantly reduce the defect density in *a*-GaN, which is crucial for the realization of high-performance devices.[16] In the present work, we demonstrate a non-polar LED with an electroluminescence (EL) wavelength of 488 nm, grown on an *a*-plane GaN buffer with an *in-situ* SiN_x interlayer. The crystalline quality and the electrical properties of GaN buffer are greatly improved by the insertion of the SiN_x interlayer. The *a*-LED shows strong and narrow emission and the peak remains constant when the injection current increases.

*Project supported by the National Natural Science Foundation of China (Grant Nos. 60676032, 60776041, 60976009 and U0834001), and the National Basic Research program of China (Grant No. 2007CB307004).

†Corresponding author. E-mail: tongju@pku.edu.cn

© 2011 Chinese Physical Society and IOP Publishing Ltd

2. Experiment and results

The a-plane GaN and LED samples were grown by the Thomas Swan metal-organic chemical deposition (MOCVD) system. Trimethylindium (TMIn), trimethylgallium (TMGa), and ammonia (NH_3), were used as In, Ga and N precursors in the epitaxy process, respectively. Bicyclopentadienyl magnesium (Cp_2Mg) and silane (SiH_4) were the sources of p-type and n-type dopants. The substrates were r-plane sapphire with $\pm 2^\circ$ surface orientation tolerance. The a-plane GaN buffer was grown by the conventional two-step growth method. First, a 150 nm thick AlN layer was grown at 1080 °C and 5300 Pa. After the AlN layer, the a-plane GaN films with 2 μm thickness were grown on r-plane sapphire substrates at 1040 °C and 10132 Pa. Then a thin SiN_x layer with a growth time of 100 s was inserted by flowing silane and ammonia. To obtain a low defect and specular surface, a 1.5 μm GaN capping layer was grown after the *in-situ* SiN_x interlayer. The growth temperature, chamber pressure and V/III ratio were kept at 1040°C, 10132 Pa and 500 during the GaN buffer growth process respectively.

Philips Material Research X-ray Diffraction (XRD) equipped with a four-crystal monochrometer was used to determine the crystallographic orientation and the crystalline quality. High resolution XRD results of the a-plane GaN buffers with and without SiN_x interlayer are shown in Fig. 1. The 2θ–ω scan of the sample presented in the inset of Fig. 1 identifies the growth surface as the $[11\bar{2}0]$ plane. The azimuthal dependences of the full width at half maximum (FWHM) of the rocking curves were measured by rotating the sample from –30° to 120° in steps of 30°. Azimuthal angles of 0° and 90° correspond to the diffraction vector of the XRD geometrically perpendicular and parallel to the c-axis, respectively. The sine-shape curve of GaN buffer without the SiN_x interlayer reveals a difference of about 0.16° between the minimum value of 0.24° (scattering plane perpendicular to c-axis of GaN) and the maximum value of 0.40° (scattering plane parallel to the c-axis). However, the in-plane FWHM anisotropies due to the hetero epitaxy process were reduced to 0.18° and 0.28° of minimum and maximum after inserting the SiN_x nanomask layer. These results indicate that the anisotropy induced by stacking faults[17] is much reduced by the insertion of the *in-situ* SiN_x interlayer and the crystalline quality of the a-plane GaN buffer is improved.

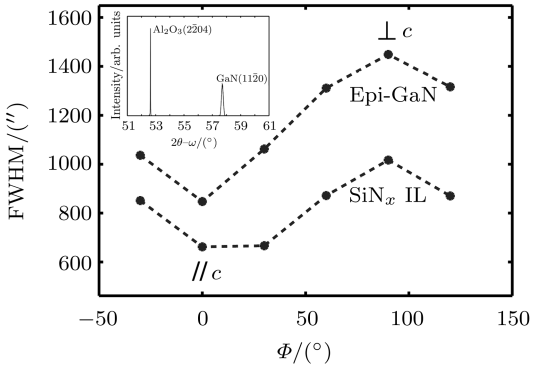
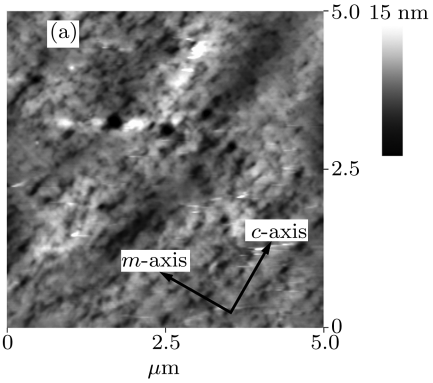


Fig. 1. HRXRD azimuthal angle dependence of the FWHMs of $(11\bar{2}0)$ rocking curves for the heteroepitaxial a-plane GaN with (SiNx IL) and without (Epi-GaN) the SiN_x interlayer on r-plane sapphire, where the inset shows 2θ–ω scan of the GaN sample.

The surface of the a-plane GaN with the SiN_x interlayer is optically specular. Figure 2 shows the AFM image and the SEM image of the a-plane GaN sample. The root-mean-square (RMS) roughness is 1.73 nm. Room temperature Hall effect measurements were also performed on the a-plane GaN buffer with the SiN_x interlayer using the Agilent HL5500 Hall System. The electrons' mobility and sheet resistance are measured to be 31.6 $cm^2/(V \cdot s)$ and 460 $\Omega/\square$, respectively. However, the a-plane GaN without the insertion of the SiN_x nanomask layer is of high resistance, and the LED structure grown on the high resistance GaN buffer does not demonstrate any electroluminescent properties. The improvement of the electrical properties of the GaN buffer could be attributed to a few causes. First, the better crystalline-quality of the GaN buffer gives rise to fewer scattering centres from defects. It could also be deduced that the resident Si atoms in the environment after growth of the SiN_x interlayer could be doped into the GaN capping layer and increase the carrier density. Another possible dopant resource is Si atoms diffusing out from the SiN_x interlayer driven by the concentration gradient.



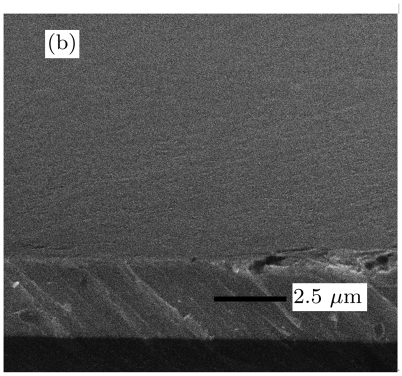


Fig. 2. (a) AFM and (b) SEM images of a-plane GaN with SiN_x interlayer surface morphology, with the SEM image taken at 15° inclined angle.

This improvement will be good for obtaining nonpolar a-plane LEDs. Figure 3 shows the structure of the LED on the GaN buffer with the SiN_x interlayer. It is comprised of a 2 μm-thick Si-doped n-GaN with an electron concentration of 2×10^{18} cm^{-3}, followed by five pairs of MQWs with 15 nm GaN barriers and 3 nm InGaN wells, and a 200 nm p-type GaN layer on the top. The p-dopant layer was activated by being annealed in nitrogen ambient at 800 °C for 20 min. Then, LED chips were fabricated by photolithography and induction-coupled plasma etching, with a size of 250 μm×600 μm. Cr/Pt/Au and Ni/Au alloys were used for n and p type Ohmic contacts, respectively.

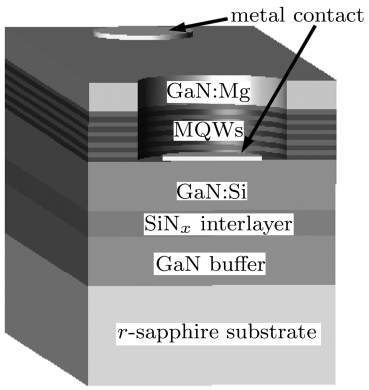


Fig. 3. A schematic representation of device structure of a-plane nonpolar LED with the SiN_x interlayer.

The room temperature EL characteristic at a forward current of 20 mA is shown in Fig. 4. The blue–green EL emission peak wavelength is 488 nm and the FWHM is 40.9 nm. The EL emission peak wavelength position was also tested as a function of forward dc current, which is shown in Fig. 5. With injection current increasing from 0 to 20 mA, the peak of emission wavelength first decreases from 507 to 488 nm. When the injection current is larger than 20 mA, peak wavelength of the a-plane LED remains constant at 488 nm. This phenomenon implies that the polarization electrical field is eliminated in such nonpolar orientation structures. The strong blueshift of the EL peak position in the initial current injection process was also reported in Ref. [10] and attributed to the filling of defect-induced band tail states.

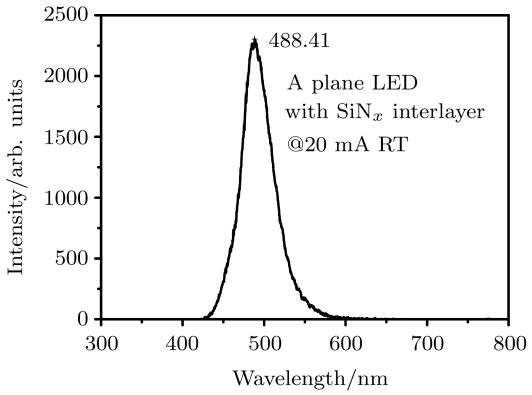


Fig. 4. EL spectrum of a-plane nonpolar LED with the SiN_x interlayer.

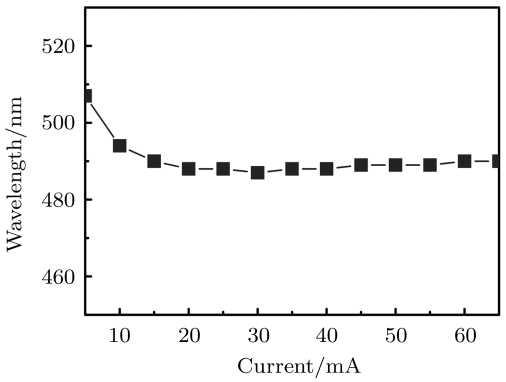


Fig. 5. EL emission peak wavelength of a-plane nonpolar LED with the SiN_x interlayer as a function of forward injection current.

3. Summary

We report on the growth and the fabrication of nonpolar a-plane LED devices with EL at a wavelength of 488 nm on a-GaN with an *in-situ* SiN_x interlayer. The SiN_x nanomask interlayer is used to improve the crystalline quality of the a-plane GaN template for nonpolar LED structures. The X-ray rocking curve FWHM of the a-plane GaN buffer is significantly decreased after the insertion of the SiN_x interlayer. The morphology of the a-plane GaN buffer remains optically specular after the growth of the GaN capping layer. Electrical properties of the nonpolar GaN

buffer are also improved. For example, the sheet resistance is reduced from high resistance to 460 Ω/□. Strong and narrow electroluminescence emissions for LED chips are demonstrated. The emission peak remains constant when the injection current increases to over 20 mA. Thus, the SiN_x interlayer in our experiment is very important for realizing *a*-plane LEDs by improving the crystalline quality and electrical properties.

Acknowledgement

A part of the experiments was carried out at the Beijing Synchrotron Radiation Facility (BSRF) of the Institute of High Energy, Chinese Academy of Sciences.

References

[1] Takeuchi T, Sota S, Katsuragawa M, Komori M, Takeuchi H, Amano H and Akasaki I 1997 *Jpn. J. Appl. Phys.* Part 2 **36** L382

[2] Miller D A B, Chemla D C, Damen T C, Grossard A C, Wiegmann W, Wood T H and Burrus C A 1985 *Phys. Rev.* B **32** 1043

[3] Bernardini F, Fiorentini V and Vanderbilt D 1997 *Phys. Rev.* B **56** R10024

[4] Im J S, Kollmer H, Off J, Sohmer A, Scholz F and Hangleiter A 1998 *Phys. Rev.* B **57** R9435

[5] Craven M D, Lim S H, Wu F, Speck J S and DenBaars S P 2002 *Appl. Phys. Lett.* **81** 469

[6] Tsuda M, Furukawa H, Honshio A, Iwaya M, Kamiyama S, Amano H and Akasaki I 2006 *Phys. Status Solidi* B **243** 1524

[7] Miyagawa R, Narukawa M, Ma B, Miyake H and Hiramatsu K 2008 *J. Cryst. Growth* **310** 4979

[8] Cui Y C, Li Y, Liu B, Mei Q, Song L H, Xie Z L, Zhang R, Zhao H and Zheng Y D 2009 *Acta Phys. Sin.* **58** 7864

[9] Craven M D, Waltereit P, Speck J S and DenBaars S P 2004 *Appl. Phys. Lett.* **84** 496

[10] Chakraborty A, Keller S, Meier C, Haskell B A, Keller S, Waltereit P, DenBaars S P, Nakamura S, Speck J S and Mishra U K 2005 *Appl. Phys. Lett.* **86** 031901

[11] Chitnis A, Chen C, Adivarahan V, Shatalov M, Kuokstis E, Mandavilli V, Yang J W and Khan M A 2004 *Appl. Phys. Lett.* **84** 3663

[12] Ling S C, Wang T C, Ko T S, Lu T C, Kuo H C and Wang S C 2008 *J. Cryst. Growth* **310** 2330

[13] Chakraborty A, Kim K C, Wu F, Speck J S, DenBaars S P and Mishra U K 2006 *Appl. Phys. Lett.* **89** 041903

[14] Kappers M J, Hollander J L, Johnston C F, McAleese C, Sridhara Rao D V, Sanchez A M, Humphreys C J, Badcock T J and Dawson P 2008 *J. Cryst. Growth* **310** 4983

[15] Ko T S, Wang T C, Huang H M, Chen J R, Chen H G, Chu C P, Lu T C, Kuo H C and Wang S C 2008 *J. Cryst. Growth* **310** 4972

[16] Hollander J L, Kappers M J, McAleese C and Humphreys C J 2008 *Appl. Phys. Lett.* **92** 101104

[17] McLaurin M B, Hirai A, Young E, Wu F and Speck J S 2002 *Jpn. J. Appl. Phys.* **41** 1348